Extended defects in the Potts-percolation model of a solid: Renormalization group and Monte Carlo analysis

H. T. Diep[1,*] and Miron Kaufman[2]

[1]*Laboratoire de Physique Théorique et Modélisation, Université de Cergy-Pontoise–CNRS, UMR 8089 2, Avenue Adolphe Chauvin, 95302 Cergy-Pontoise Cedex, France*
[2]*Department of Physics, Cleveland State University, Cleveland, Ohio 44115, USA*

We extend the model of a 2*d* solid to include a line of defects. Neighboring atoms on the defect line are connected by springs of different strength and different cohesive energy with respect to the rest of the system. Using the Migdal-Kadanoff renormalization group we show that the elastic energy is an irrelevant field at the bulk critical point. For zero elastic energy this model reduces to the Potts model. By using Monte Carlo simulations of the three- and four-state Potts model on a square lattice with a line of defects, we confirm the renormalization-group prediction that for a defect interaction larger than the bulk interaction the order parameter of the defect line changes discontinuously while the defect energy varies continuously as a function of temperature at the bulk critical temperature.

I. INTRODUCTION

Thermodynamics of solids with defects is a topic of current interest [1,2]. In this paper we expand an equilibrium statistical mechanics model [3] of a solid to include extended defects. Previously we used [4] the realistic anharmonic energy versus atomic distance developed by Ferrante and Smith [5] in a mean-field-type computation. We then evaluated [6] the role of thermal fluctuations by using renormalization-group and Monte Carlo simulations.

In our model described in Sec. II, the solid is constituted of harmonic springs. If the energy of such a spring is larger than a threshold, the spring is likely to fail [7]. In the limit of zero elastic energy the model reduces to the Potts model [8], which has been used to describe correlated and uncorrelated percolation processes [9–12].

In Sec. III we present phase diagrams based on the renormalization-group Migdal-Kadanoff scheme. This scheme is of course an approximation for models on regular lattices but as demonstrated by Berker and Ostlund [13] it is exact for hierarchical lattices. This latter feature and its simplicity make the Migdal-Kadanoff scheme quite popular [14–19]. We analyze the stability of fixed points and find that the elastic energy is an irrelevant field in the renormalization-group sense. For this reason, in Sec. IV we report Monte Carlo simulations of the model with zero elastic energy, i.e., Potts model on a square lattice with a defect line. Our goal is to verify the renormalization-group prediction [20] that for $q=3,4$, on the defect line, at the bulk critical temperature, the order parameter jumps discontinuously from zero (high temperature phase) to a nonzero value (low temperature phase) while the energy varies continuously with temperature. This is interesting since for those q values the bulk transition is continuous. It was argued [20] that this unusual 1*d* defect transition is due to the infinite range correlations at the bulk critical point. It resembles the Thouless

transition [21,22] in a one-dimensional system with inverse squared distance decaying interactions. A scaling theory of this defect transition has also been proposed [23]. Our concluding remarks are found in Sec. V.

II. MODEL

The solid is made of "springs" some of which are alive and some are failed upon thermal excitations. All processes are assumed to be reversible, unlike the work of Beale and Srolovitz [24] where springs fail irreversibly. The energy of a spring $\langle i,j \rangle$ is given by the Hooke law,

$$H_{ij} = -E_C + \frac{k}{2}(\vec{r}_i - \vec{r}_j)^2, \tag{1}$$

where $\vec{r}_i$ is the displacement vector from the equilibrium position of atom i, E_C is the cohesive energy, k is elastic constant, and a is the equilibrium lattice spacing. If the energy of the spring is larger than the threshold energy E_0 the spring is more likely to fail than to be alive. p is the probability that the spring is alive and $1-p$ the probability that the spring breaks. We assume its dependence on energy to be given by the Boltzmann weight,

$$\frac{p}{1-p} = e^{-(\mathcal{H}-E_0)/k_B T} = w e^{-K/2(\vec{r}_i - \vec{r}_j)^2}, \tag{2}$$

where $K = k/k_B T$ and $w = e^{(E_C + E_0)/k_B T}$.

For the extended line of defects the elastic, cohesive, and threshold energies may take values different from the rest of the system. Hence, while in the bulk the parameters are K and w; on the line of defects they are K_d and w_d.

We allow for correlations between failing events by using the Potts number of states q, which plays the role of a fugacity controlling the number of clusters. For $q=1$ we have random percolation as springs fail independently. When comparing configurations that have the same number of live springs B, the configuration with higher number of clusters C is more probable if $q>1$ and less probable if $q<1$. The

*Corresponding author; diep@u-cergy.fr

partition function is a sum over all possible configurations of "live" springs:

$$Z = \sum_{config} q^c w^B Z_{\text{elastic}}^{\text{config}}. \qquad (3)$$

C is the number of clusters, including single site clusters, and B is the number of live springs. The restricted partition function associated with the elastic energy for a given configuration of bonds (live springs) is

$$Z_{\text{elastic}}^{\text{config}} = \text{Tr}_r \, e^{-H_{\text{elastic}}/k_B T}, \qquad (4)$$

$$-\frac{H_{\text{elastic}}}{k_B T} = \sum_{\langle i,j \rangle} \frac{K}{2} (\vec{r}_i - \vec{r}_j)^2. \qquad (5)$$

In Eq. (5) the sum is over all live springs.

By using the Kasteleyn-Fortuin expansion [25] for Potts model we can rewrite the partition function as

$$Z = \text{Tr}_\sigma \, \text{Tr}_r \, e^{-\mathcal{H}/k_B T}. \qquad (6)$$

The Hamiltonian is

$$-\frac{\mathcal{H}}{k_B T} = \sum_{\langle i,j \rangle} \left[J_1 \delta(\sigma_i, \sigma_j) - \frac{J_2}{2} \delta(\sigma_i, \sigma_j)(\vec{r}_i - \vec{r}_j)^2 \right]$$
$$+ \sum_{\langle i,j \rangle defect} \left[J_{1d} \delta(\sigma_i, \sigma_j) - \frac{J_{2d}}{2} \delta(\sigma_i, \sigma_j)(\vec{r}_i - \vec{r}_j)^2 \right], \qquad (7)$$

where σ_i is a Potts spin taking q values. This mapping is a Gaussian approximation valid when, on the right-hand side of Eq. (7), the elastic energy is small compared to the first energy contribution. In our Monte Carlo simulations, we use the Hamiltonian in Eq. (7) for integer values of q. The coupling constants J_1 and J_2 are related to the original parameters, w and K, as follows:

$$J_1 = \ln(1 + w), \qquad (8)$$

$$J_2 = K \frac{w}{w + 1}, \qquad (9)$$

$$J_{1d} = \ln(1 + w_d), \qquad (10)$$

$$J_{2d} = K_d \frac{w_d}{w_d + 1}. \qquad (11)$$

Compressible Ising models, with Hamiltonians somewhat similar to Eq. (7), have been reviewed by Landau *et al.* [26].

III. RENORMALIZATION GROUP

The Migdal-Kadanoff recursion equations [27,28] for two dimensions are obtained by assuming that each atom coordinate varies in the interval $(-1/2, 1/2)$, where the equilibrium lattice constant is 1, and also using the Gaussian approximation (small elastic energy):
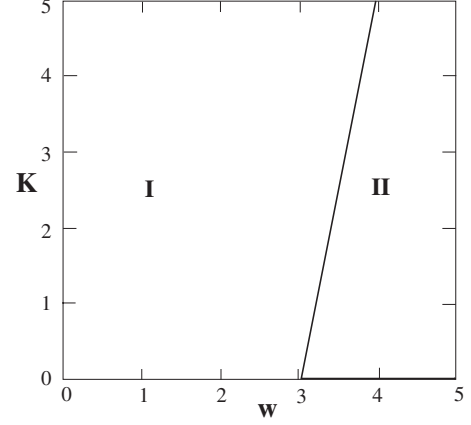
$$w' = [1 + U(w, K, q)]^2 - 1, \qquad (12)$$

FIG. 1. Bulk phase diagram for $q = 10$ in the plane (w, K). Potts critical line separates phase (i) with many failed springs from phase (II) with many live springs.

$$K'w' = K[1 + U(w, K, q)]U(w, K, q), \qquad (13)$$

$$w'_d = [1 + U(w, K, q)][1 + U(w_d, K_d, q)] - 1, \qquad (14)$$

$$K'_d w'_d = \frac{1}{2} K_d [1 + U(w, K, q)] U(w_d, K_d, q)$$
$$+ \frac{1}{2} K [1 + U(w_d, K_d, q)] U(w, K, q), \qquad (15)$$

where

$$U(w, K, q) = \frac{w^2 \, \text{erf}(\sqrt{K/4})}{q\sqrt{K/\pi} + \sqrt{8}w \, \text{erf}(\sqrt{K/8})}. \qquad (16)$$

The above recursion equations represent the Gaussian approximation of the exact solutions for hierarchical lattices. The renormalization-group flows in the bulk parameter space (w, K) are governed by the following fixed points at $K = 0$ (pure Potts model):

(i) $w = 0$ (nonpercolating live springs);

(ii) $w = \infty$ (percolating network of live springs);

(iii) $w = w_c$ (Potts critical point).

A stability analysis at the bulk Potts critical point ($K = 0$, $w = w_c$) yields the following two eigenvalues:

(i) the thermal eigenvalue: Λ_1 (for the direction along the $K = 0$ axis) is always larger than 1, meaning the $w - w_c$ is a relevant field;

(ii) the other eigenvalue associated with the flow along the $w = w_c$ line away from the pure model ($K = 0$) is $\Lambda_2 < 1$ for all q. This means that there is a line of points in the (w, K) flowing into, and thus is in the same universality class as, the pure Potts critical point $(w_c, 0)$.

The bulk phase diagram (Fig. 1), for any given q, in the (w, K) plane shows two phases: (1) "crumbling" solid with many failed springs and (2) solid with mostly live springs. The two phases are separated by a critical line in the universality class of the q-state Potts model.

The defect fixed points are obtained from Eqs. (14) and (15) after setting the bulk fields w and K at their fixed point values (bulk material is critical): $w = w_c$, $K = 0$. All the fixed
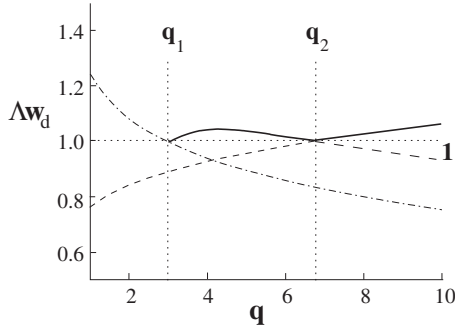
FIG. 2. Renormalization-group eigenvalue Λw_d vs q: solid line at defect critical fixed point; dotted-dashed line at the percolating critical fixed point; dashed line at the nonpercolating fixed point. Two vertical lines are $q_1 = 3$ and $q_2 = 6.8$ (see text for comments).

points are obtained for $K_d = 0$. We find fixed points at $w_d = \infty$ and at $w_d = w_c$ for all q. For $q > q_1 = 3$ a third fixed point emerges from the one at $w_d = \infty$ at $w_d = w*$. At $q = q_2 = 6.8$ (when exponent $\alpha = 0$) the two finite w_d fixed points exchange position.

The stability of the fixed points for perturbations of the defect fields (w_d, K_d) is determined by the following:

(i) the eigenvalue Λw_d governing flow along $K_d = 0$ axis is larger than unity (i.e., relevant perturbation) at the fixed point $K_d = 0$, $w_d = \max(w_c, w*)$ and is less than unity (i.e., irrelevant perturbation) at the fixed point $K_d = 0$, $w_d = \min(w_c, w*)$ (Fig. 2);

(ii) the eigenvalue $\Lambda K_d < 1$ for all fixed points (Fig. 3).

The defect phase diagram (Fig. 4) represented in the plane (w_d, K_d) is obtained for the bulk fields at their critical values: $w = w_c$, $K = 0$. The plane (w_d, K_d) is divided in two regions by a critical line that flows into the fixed point: $w_d = \max(w_c, w*)$, $K_d = 0$. To the right of it (large w_d), the live springs on the defect line are percolating, i.e., the Potts order parameter is nonzero on the defect line even though in the bulk it is zero. All points in that region flow to the fixed point $w_d = \infty$, $K_d = 0$. The phase to the left of the critical line (small w_d) is governed by the fixed point at $w_d = \min(w_c, w*)$, $K_d = 0$.

Since the elastic energy is irrelevant renormalization group (RG) field, we concentrate next on the $K = K_d = 0$ case.
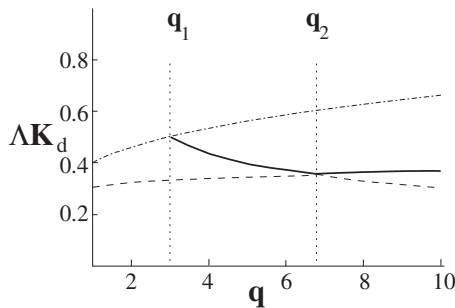

FIG. 3. Renormalization-group eigenvalue ΛK_d vs q: solid line at defect critical fixed point; dashed-dotted line at the percolating critical fixed point; dashed line at the nonpercolating fixed point. Since these eigenvalues are less than unity, the elastic energy is an irrelevant field at the three fixed points. Two vertical lines are $q_1 = 3$ and $q_2 = 6.8$ (see text for comments).
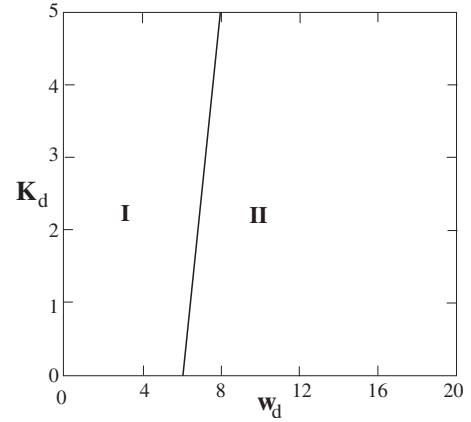

FIG. 4. Phase diagram at $w = w_c$, $K = 0$ in plane (w_d, K_d). The two critical phases (infinite correlation length) are separated by a defect critical line. In the small w_d phase (I) there is zero probability for percolation on the defect line, while in the large w_d phase (II) there is a finite probability for percolation on the defect line.

The RG analysis [20] of this problem (two-dimensional Potts model with a defect line) predicts for $2 < q \leq 4$ a hybrid phase transition on the defect line: discontinuous order parameter and continuous energy. The defect crossover exponent is [29] $\Phi = 1 - \nu$, so $\Phi = 0$ with continuously varying defect exponents in the $q = 2$ case (for hierarchical lattice this is $q = 6.8$), while for $q > 2$ the crossover exponent is positive, signaling crossovers to other universality classes: hybrid (discontinuous) transition for strong defect coupling and new universality class for weak defect coupling.

IV. MONTE CARLO SIMULATIONS

In this section since we set the elastic couplings to zero in Eq. (7), we perform MC simulation of the Hamiltonian

$$-\frac{\mathcal{H}}{k_B T} = J \sum_{\langle i,j \rangle} \delta(\sigma_i, \sigma_j) + J_d \sum_{\langle i,j \rangle defect} \delta(\sigma_i, \sigma_j), \qquad (17)$$

where J is the interaction parameter between the bulk nearest neighbors (NN) and J_d is that between two NN on the defect line [J is equal to J_1 of Eq. (8), and J_d is J_{1d} of Eq. (10)].

We consider a square lattice of size $N_x \times N_y$ where $N_x = 80, 120, 160, 200, \ldots, 1920$ and $N_y = 40, 60, 80$. Each lattice site is occupied by a q-state Potts spin. We place the defect line at the middle of the y side of the sample, i.e., $y = N_y/2$. The length of the defect line is thus N_x. The reason why we use a very long length for the defect line stems from the fact that the determination of a transition in a linear chain needs large enough sizes to avoid statistical fluctuations. We use periodic boundary conditions.

Our purpose here is to test the following RG prediction of the previous section: at the bulk transition temperature T_c, the defect line undergoes a phase transition where its order parameter is discontinuous but its energy is continuous. The bulk transition temperature is the temperature at which the phase transition of the system without the defect line takes place.

Let us consider the case where $q = 4$. The critical temperature is given by the exact formula $(k_B T_c/J)^{-1} = \ln(1 + \sqrt{q})$.
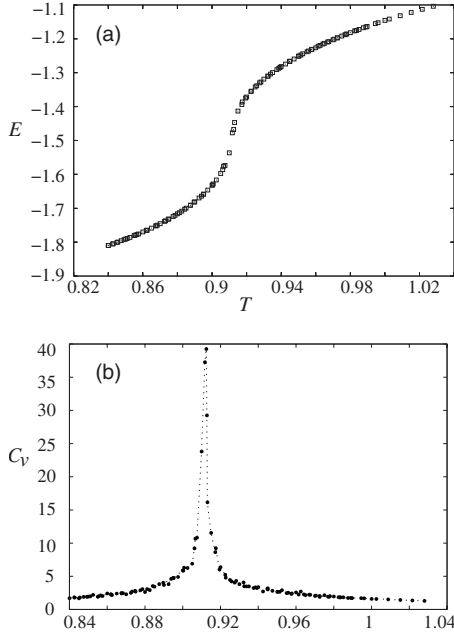
FIG. 5. Case without defects: energy per spin E (upper curve) and specific heat per spin C_v (lower curve; line is a guide for the eyes) vs temperature T for $q=4$, with $N_x=1920$, $N_y=60$, and $J_d=J=1$.

With $q=4$, one has $T_c \simeq 0.910\ 239$ in units of J/k_B. Note that this value of T_c corresponds to the thermodynamic limit, i.e., infinite system size. In MC simulation, we work at finite sizes, so for each size we have to determine the "pseudo" transition which corresponds in general to the maximum of the specific heat or of the susceptibility. The maxima of these quantities need not to be at the same temperature. Only at the infinite size, they should coincide. The theory of finite-size scaling permits to deduce properties of a system at its thermodynamic limit. We have used in this work a size large enough to reproduce the bulk transition temperature up to the fourth decimal.

In order to determine the nature of the phase transition of the defect line, we shall use the histogram technique [30] which is known to allow us to distinguish with accuracy the order of the phase transition.

The simulation is carried out as follows. We fix $J=1$ hereafter. For each value of J_d, using first the standard Metropolis
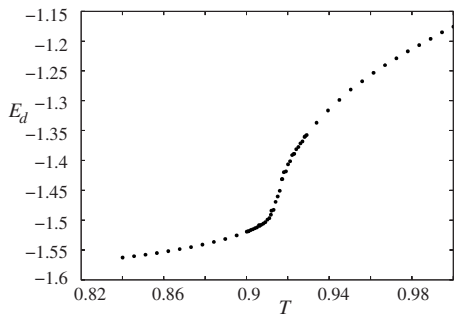

FIG. 6. Energy per spin E_d of the defect line vs temperature T for $q=4$, $J_d=1.6$ with $N_x=1920$, $N_y=60$ and $J=1$. Note that E_d is continuous at T_c. See text for comments.
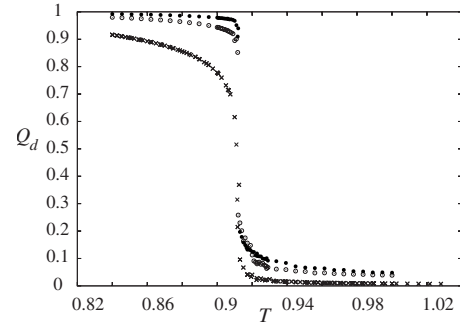

FIG. 7. Order parameters Q_d of the defect line for $J_d=2$ (upper curve with black circles), $J_d=1.6$ (middle curve with void circles) and bulk order parameter Q (lower curve with crosses) vs temperature T for $q=4$ with $N_x=1920$, $N_y=60$, and $J=1$. Note that Q_d is discontinuous at T_c. See text for comments.

MC method [31] we equilibrate the system of a given size $N_x \times N_y$ at a given temperature T during 10^6 Monte Carlo sweeps (MCS) per spin before averaging physical quantities over the next 2×10^6 MCS. We determine the transition temperature at the given size $N_x \times N_y$ by examining the calculated physical quantities such as the internal energy per spin E, the specific heat C_v per spin, the Potts order parameter Q, and the susceptibility per spin χ. For the bulk q-state Potts model, Q is defined as

$$Q = \frac{q \max(Q_1, Q_2, \ldots, Q_q) - 1}{q - 1}, \tag{18}$$

where $Q_i = n_i/(N_x \times N_y)$ $(i=1,\ldots,q)$, n_i being the number of sites having q_i. For the defect line, the order parameter Q_d is similarly defined on the defect line, namely,

$$Q_d = \frac{q \max(Q'_1, Q'_2, \ldots, Q'_q) - 1}{q - 1}, \tag{19}$$

where $Q'_i = n'_i/N_x$ $(i=1,\ldots,q)$, n'_i being the number of sites on the defect line having q_i.

Let us show first in Fig. 5 the energy and the specific heat of the case without defects where the bulk critical temperature is $T_c \simeq 0.9103$ for $q=4$ with the size used here (the exact value of T_c is 0.910 239). The energy of the defect line is shown in Fig. 6.
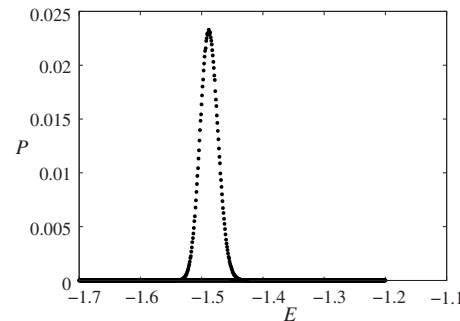

FIG. 8. Energy histogram of the defect line taken at T_c for $q=4$, $J_d=1.6$ with $N_x=1920$, $N_y=60$, and $J=1$. See text for comments.
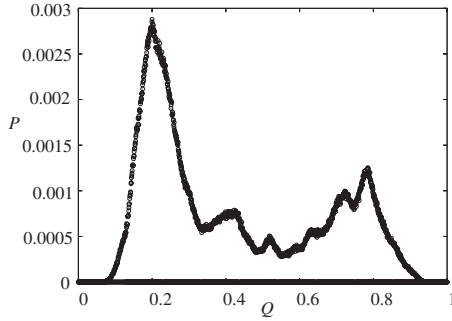
FIG. 9. Histogram of the order parameter Q_d taken at T_c for q =4, J_d=1.6 with N_x=1920, N_y=60, and J=1. Note the double-peak structure indicating that Q_d is discontinuous at T_c. See text for comments.

The order parameters of the bulk and of the defect line are shown in Fig. 7 for q=4, J=1 and J_d=1.6 and 2.

These figures show that at the "bulk" phase transition temperature T_c=0.9103, while the defect energy is continuous, the order parameter of the defect line undergoes a vertical fall, indicating a discontinuity predicted by the RG analysis shown in the previous section. For large values of J_d, for instance J_d=2, the defect line takes a very long time to become disordered for T slightly larger than T_c. Several million MC sweeps are necessary.

In order to check the behaviors of E_d and Q_d at T_c, we have calculated the defect energy histogram not only at T_c but also in the temperature region around T_c. As it turned out, we observe only a Gaussian distribution of E_d (see Fig. 8 confirming the absence of discontinuity of E_d). Note that if the energy is discontinuous, its histogram should show a double-peak structure, not a Gaussian one.

We have also established a histogram for Q_d in the following manner. We divided the interval between 0 and 1 into N_x intervals. At each MC sweep, we added 1 in the interval corresponding to the value of Q_d. In doing so for 2 million MC sweeps, we obtained a histogram for Q_d which is shown in Fig. 9 at T_c. As seen, we have a double-peak distribution of Q_d indicating that during the time the defect line can have both the ordered and disordered phases. This is a strong signature of the discontinuity of Q_d.
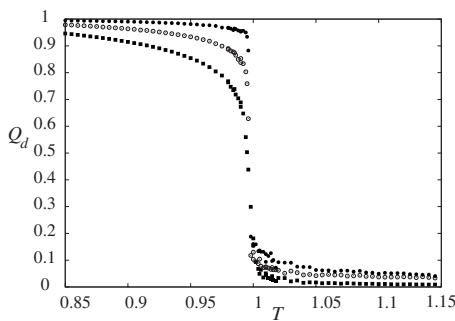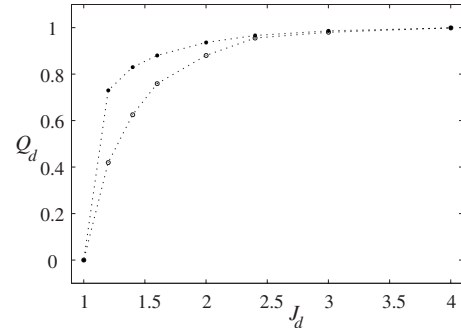

FIG. 11. Value of the order parameter Q_d taken at T_c versus J_d for q=4 (upper curve) and q=3 (lower curve) with N_x=1920, N_y =60, and J=1. Lines are guides for the eyes.

Note that the size effects for N_y=40, 60, 80, and 100 are not significant and are included in the error estimation. Simulations have been carried out also for other values of J_d between 1.2 and 4. The results show the same aspects as those shown above with J_d=1.6.

Now, let us examine the case where q=3. The results are very similar to the case q=4 shown above. So the conjecture of the RG analysis where the transition of the defect line is of first order for J_q>J at T_c for q>2 is verified here. Figure 10 shows the defect order parameter Q_d versus T for q=3 with several values of J_d. Note that T_c=0.9949 for q=3.

Let us show in Fig. 11 the value of Q_d taken at T_c as a function of J_d. As seen, the gap is increased with increasing J_d.

At this stage, it is worth to mention that due to the usual finite-size effect, the order parameters Q and Q_d do not vanish above T_c: a finite tail exists and decreases with increasing lattice size. For Q, the transition point is, in simulations, taken at the change of curvature of Q, i.e., at the maximum of the corresponding susceptibility. As for Q_d, due to its discontinuity at T_c, the values shown in Fig. 11 are the upper one at T_c. For clarity, the error bars are not shown there, but it is on the second digit, for instance Q_d=0.880 ± 0.020 for J_d=1.6.

We show now the time dependence of the order parameter Q_d and the energy. Figures 12 and 13 show these quantities for J_d=2 at T_c=0.9949 and at a temperature slightly above
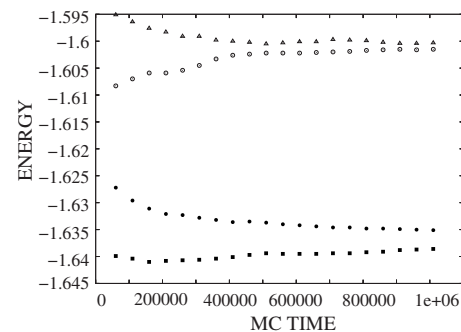

FIG. 10. Order parameters Q_d of the defect line for J_d=2 (upper curve with black circles), J_d=1.4 (middle curve with void circles) and bulk order parameter Q (lower curve with black squares) vs temperature T for q=3 with N_x=1920, N_y=60, and J=1. Note that Q_d is discontinuous at T_c. See text for comments.

FIG. 12. Time dependence of the energy per spin of the defect line for q=3 with J_d=2 at T_c=0.9949 and at T=1. From the bottom: heating to T_c, cooling to T_c, heating to T=1, cooling to T=1. See text for comments.
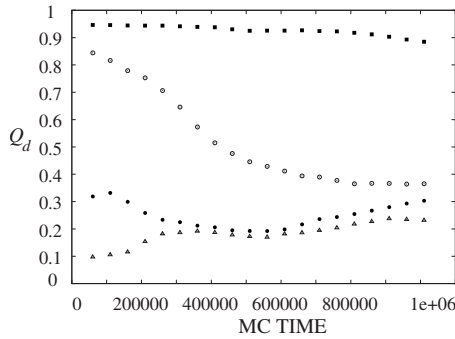
FIG. 13. Time dependence of the order parameters Q_d of the defect line for $q=3$ with $J_d=2$ at $T_c=0.9949$ and at $T=1$. From the top: heating to T_c, heating to $T=1$, cooling to T_c, cooling to $T=1$. See text for comments.

T_c, namely, $T=1$. Two procedures have been used: (i) heating, i.e., using the ordered phase (F) as initial spin state; (ii) cooling, i.e., using a paramagnetic state (P) as initial condition. We discuss first the energy case. At T_c, heating from the F state (bottom curve in Fig. 12) and cooling from the P state (second curve from the bottom in Fig. 12) give the same energy only after two million MC steps/spin (see the first million MC steps in Fig. 12). At $T=1$, one needs almost the same MC time to get the same energy for the heating and cooling (curves 3 and 4 from the bottom in Fig. 12).

The time dependence of Q_d is interesting (Fig. 13):

(i) At T_c, Q_d with F condition stays stable (first curve from top in Fig. 13) and reaches the stationary value 0.88 at two million MC steps/spin. This means that the defect line is ordered at T_c while the bulk spins are disordered. However, when cooled from the P state (third curve from the top), Q_d stays very small (disordered state). We conclude that at T_c there are two possible values of Q_d for the same energy. This explains the gap of Q_d at T_c shown earlier.

(ii) At $T=1$, slightly above T_c, Q_d takes a long time ($\simeq 500\,000$ MC step/spin) to become disordered in the heating procedure (second curve from the top) while it is disordered all the way in the cooling procedure.

Let us discuss more about the discontinuity of the order parameter Q_d at T_c. In a standard first-order transition, the ordered and disordered phases coexist at T_c yielding a discontinuity in both energy and order parameter. In the case studied here, only Q_d is discontinuous, while E_d is not. Thus, there is no double-peak energy distribution. To answer the question how Q_d can take two values at T_c, we have examined the snapshots of the defect line taken during the simulation time. Interesting enough, we observed configurations schematically of the types:

(i) 111111..1111111..111111.. where dots indicate Potts values other than 1 (same kind of ordered segments separated by disordered portions);

(ii) 111111..3333333..222222.. (random ordered segments separated by disordered portions).

It is obvious that these configurations give the same energy if the number of disordered portions is the same, while Q_d is different: the first configuration yields a large value of Q_d and the second a zero one. This observation explains why at T_c the energy is continuous but the order parameter is not.

The phase transition observed here for the defect line is very interesting in several aspects:

(i) the nature of the transition is novel in the sense that only the defect order parameter is discontinuous, not the defect energy, nor the bulk order parameter and bulk energy;

(ii) note that long-range interaction in one dimension can cause a first-order transition [32,33], while systems with short-range interaction do not show such a phase transition. The present defect line with NN interaction shows thus an exception. We believe that its immersion in disordered neighboring lines at T_c plays a key role in provoking such a pseudodiscontinuous transition.

V. CONCLUSIONS

In this paper we have studied a model of a two-dimensional solid with an extended defect line using the Migdal-Kadanoff renormalization group. Since the elastic energy turns out to be an irrelevant field, we then studied this model for zero elastic energy, i.e., $2d$ Potts model with a defect line, using Monte Carlo simulations. The renormalization-group analysis of the Potts model on a $2d$ hierarchical lattice with a defect line suggests an interesting behavior at the bulk transition T_c if the interaction on the defect line J_d is larger than the bulk interaction J: the order parameter of the defect line should undergo a discontinuity at T_c while the energy is continuous. Our Monte Carlo simulations of the three- and four-state Potts model on the square lattice with a defect line confirm the RG prediction.

To conclude, we would like to emphasize two points of interest. First, the existence of a phase transition in a one-dimensional system (defect line) is rare. It is induced by the bulk infinite correlations at criticality. Second, the nature of the phase transition is unusual in the sense that the order parameter is discontinuous while the energy is not. This is somewhat similar to the Thouless transition [21] in $1d$ models with long-range interactions.

[1] L. Gomez, A. Dobry, C. Geuting, H. T. Diep, and L. Burakovsky, Phys. Rev. Lett. **90**, 095701 (2003).

[2] Z. Y. Man, Y. W. Zhang, and D. J. Srolovitz, Comput. Mater. Sci. **44**, 86 (2008).

[3] Robin L. Blumberg Selinger, Z. G. Wang, W. M. Gelbart, and A. Ben-Shaul, Phys. Rev. A **43**, 4396 (1991).

[4] M. Kaufman and J. Ferrante, NASA Tech. Memo. 107112 (1996).

[5] J. Ferrante and J. R. Smith, Phys. Rev. B **31**, 3427 (1985).

[6] M. Kaufman and H. T. Diep, J. Phys.: Condens. Matter **20**, 075222 (2008).

[7] G. N. Hassold and D. J. Srolovitz, Phys. Rev. B **39**, 9273 (1989).

[8] R. B. Potts, Proc. Camb. Philos. Soc. **48**, 106 (1952).

[9] F. Y. Wu, Rev. Mod. Phys. **54**, 235 (1982).

[10] M. Kaufman and D. Andelman, Phys. Rev. B **29**, 4010 (1984).

[11] M. Kaufman and M. Kardar, Phys. Rev. B **29**, 5053 (1984).

[12] V. A. Ivanskoi, Tech. Phys. **53**, 455 (2008).

[13] A. N. Berker and S. Ostlund, J. Phys. C **12**, 4961 (1979).

[14] R. B. Griffiths and M. Kaufman, Phys. Rev. B **26**, 5022 (1982).

[15] M. Kaufman and K. K. Mon, Phys. Rev. B **29**, 1451 (1984).

[16] M. Kaufman and R. B. Griffiths, Phys. Rev. B **30**, 244 (1984).

[17] A. Erbas, A. Tuncer, B. Yucesoy, and A. N. Berker, Phys. Rev. E **72**, 026129 (2005).

[18] C. Guven, A. N. Berker, M. Hinczewski, and H. Nishimori, Phys. Rev. E **77**, 061110 (2008).

[19] M. Hinczewski and A. N. Berker, Phys. Rev. E **73**, 066126 (2006).

[20] M. Kaufman and R. B. Griffiths, Phys. Rev. B **26**, 5282 (1982).

[21] D. J. Thouless, Phys. Rev. **187**, 732 (1969).

[22] M. Aizenman, J. T. Chayes, L. Chayes, and C. M. Newman, J. Stat. Phys. **50**, 1 (1988).

[23] F. Igloi and L. Turban, Phys. Rev. B **47**, 3404 (1993).

[24] P. D. Beale and D. J. Srolovitz, Phys. Rev. B **37**, 5500 (1988).

[25] C. M. Fortuin and P. W. Kasteleyn, J. Phys. Soc. Jpn. Suppl. **26**, 11 (1969).

[26] D. P. Landau, B. Dunweg, M. Laradji, F. Tavazza, J. Adler, L. Cannavacioullo, and X. Zhu, Lect. Notes Phys. **704**, 127 (2006).

[27] A. A. Migdal, Sov. Phys. JETP **42**, 743 (1976).

[28] L. P. Kadanoff, Ann. Phys. (N.Y.) **100**, 359 (1976).

[29] T. W. Burkhardt and E. Eisenriegler, Phys. Rev. B **24**, 1236 (1981).

[30] A. M. Ferrenberg and R. H. Swendsen, Phys. Rev. Lett. **61**, 2635 (1988); A. M. Ferrenberg and D. P. Landau, Phys. Rev. B **44**, 5081 (1991).

[31] K. Binder and D. W. Heermann, *Monte Carlo Simulation in Statistical Physics* (Springer, New York, 2002).

[32] S. Reynal and H. T. Diep, Phys. Rev. E **72**, 056710 (2005).

[33] S. Reynal and H. T. Diep, Phys. Rev. E **69**, 026109 (2004).